

Tensor interaction in coherent elastic neutrino-nucleus scattering

Jiajun Liao,^{1,*} Jian Tang,^{1,†} and Bing-Long Zhang^{1,‡}

¹*School of Physics, Sun Yat-sen University, Guangzhou, 510275, China*

Neutrino tensor interactions have gained prominence in the study of coherent elastic neutrino-nucleus scattering (CE ν NS) recently. We perform a systematical examination of the nuclear effect, which plays a crucial role in evaluating the cross section of CE ν NS in the presence of tensor interactions. Our analysis reveals that the CE ν NS cross section induced by tensor interactions is not entirely nuclear spin-suppressed and can be enhanced by a few orders of magnitude compared to the conventional studies. The neutrino magnetic moment induced by the loop effect of tensor interactions, is also taken into account due to its sizable contribution to the CE ν NS cross section. We also employ data from the COHERENT experiment and recent observations of solar ⁸B neutrinos from dark matter direct detection experiments to scrutinize the parameter space of neutrino tensor interactions.

Introduction. The discovery of the neutrino oscillation clearly indicates the existence of new physics beyond the standard model (SM), triggering substantial theoretical and experimental efforts to explore the nature of neutrinos. A model-independent way to explore new physics in the neutrino sector is parameterized in the form of generalized neutrino interactions [1–4], i.e., four fermion operators with scalar, pseudo-scalar, vector, axial-vector and tensor Lorentz-invariant structures. Among these interactions, the tensor interactions historically received comparatively less attention but attracted numerous interests in the literature in recent years. Neutrino tensor interactions can arise from lepto-quark models [5, 6], SM effective field theory [7, 8], and unparticle physics models [9]. The parameter space of tensor interactions has been explored by diverse phenomenological channels, including deep inelastic scattering [8, 10, 11], muon decay [12, 13], neutrino mass [14, 15], β decay [16–21], etc.

Recent observations of the coherent elastic neutrino-nucleus scattering process provide a novel probe to new physics in the neutrino sector [22]. The first observation of SM CE ν NS was achieved in 2017 by the COHERENT collaboration through an accelerator-based experiment [23], confirmed by subsequent experiments [24, 25], and the first indication of solar ⁸B neutrinos induced CE ν NS events in the DM direct detection (DD) experiments was also reported by PandaX-4T [26] and XENONnT [27] in 2024. The SM CE ν NS process [28], arising from the exchange of a vector Z boson, is well understood in theory based on the point nucleus assumption (PNA). In the PNA, a nucleus is treated as a point particle carrying a charge and a spin, leading to exclusive spin-independent (SI) and spin-dependent (SD) interactions, with which the nuclear effects can be encoded into SI and SD form factors. In particular, the nuclear effect of the SM CE ν NS process is encoded a SI form factor, describing the weak charge distribution within a nucleus. Due to the success of PNA in the SM, most studies on tensor interactions to simply adopt the same formalism as in the vector case, using an identical form factor to describe the nuclear effect [3, 4, 8, 9, 29–37]. However, extensive studies on

dark matter (DM) effective field theory reveal that the nucleus should be modeled by a collective nucleon system, leading to extra internal interactions between a point particle and a nucleus after the matching between relativistic interactions and non-relativistic (NR) nucleon operators [38, 39]. This procedure usually adopts a complete set of six nuclear response functions instead of the conventional SI/SD form factors used in the elastic scattering. The nuclear response functions reveal the charge or current distribution inside the nucleus, depending on the underlying interactions and the corresponding nucleon operators. Therefore, it is natural to go beyond the PNA and utilize the nuclear response functions to evaluate the nuclear effect for tensor interactions.

Previous studies in the nuclear response framework [40, 41] simply assumed that the primary contribution originates from the spin operator \vec{s}_N derived by matching the tensor interactions into the NR operators. Consequently, the nuclear effect is encoded into two nuclear response functions of the spin operator $\vec{\sigma}_N$, resulting in a suppression of several orders of magnitude in the cross sections relative to those in the PNA. This significant suppression arises from the nuclear response functions, because the amplitude for a neutrino scattering off paired nucleons with opposite spin directions cancel with each other. This approach was overlooked for a long time but recently has been utilized in several phenomenological studies [42–44]. Nonetheless, we find that this result is based on naive power counting (NPC), indicating that other essentially dominant nucleon operators might be ignored due to a suppression from the ratio of the momentum transfer to the nucleon mass, i.e., $|\vec{q}|/m_N$, which is typically $\mathcal{O}(0.01)$. For the unit operator 1_N , omitted in the NPC procedure, the amplitude for a neutrino scattering off a nucleus is the coherent sum of those from each individual nucleon. This coherent enhancement effect compensates the suppression factor, and simultaneously amplifies the effect of the other operator through the interference with 1_N .

In this Letter, we systematically investigate the tensor interactions in CE ν NS in light of the nuclear response framework. The cross section can be decomposed into

parity-odd and parity-even components, stemming from the nucleon operators suppressed by $|\vec{q}|/m_N$ and $\vec{\sigma}_N$, respectively. We find that the NPC results only contain the parity-even part, and the dominant contribution to the cross section originates from the parity-odd part, which exhibits no nuclear spin suppression and is coherently enhanced, thus yields a few orders of magnitude improvement over the NPC results. We also discuss the sizable contribution to the CE ν NS cross section from the neutrino magnetic moment (ν MM) induced by a loop diagram of the tensor interactions [6, 45]. In addition, we perform phenomenological investigations based on the data from the well-measured COHERENT experiment and recent solar ^8B neutrino observations in the DM DD experiments at PandaX-4T and XENONnT.

Theoretical framework. The neutral tensor interactions between quarks q and neutrinos ν_α can be described by:

$$\mathcal{L}_{\text{eff}}^T = \sum_{q=u,d} \sum_{\alpha=e,\mu,\tau} G_{T,\alpha}^q (\bar{\nu}_\alpha \sigma^{\mu\nu} \nu_\alpha) (\bar{q} \sigma_{\mu\nu} q), \quad (1)$$

with $\sigma^{\mu\nu} \equiv \frac{i}{2}[\gamma^\mu, \gamma^\nu]$. Nucleons, rather than quarks, serve as the effective hadronic degrees of freedom in describing low-energy scattering processes. Transitioning from quarks to nucleons can be achieved via the tensor interaction's nucleon matrix element [41]:

$$\langle N_{p'} | \bar{q} \sigma^{\mu\nu} q | N_p \rangle = \bar{u}_{p'} \left[\sigma^{\mu\nu} F_{1,T}^{q,N} - \frac{i}{m_N} (\gamma^\mu q^\nu - \gamma^\nu q^\mu) F_{2,T}^{q,N} \right] u_p, \quad (2)$$

where nucleon form factors evaluated at zero momentum transfer $F_{1,T}^{u,p} = 0.784(28)$ and $F_{1,T}^{d,p} = -0.204(11)$ [46] are relative to the tensor charges, and $F_{2,T}^{u,p} = -1.5(1.0)$ and $F_{2,T}^{d,p} = 0.5(3)$ [47] are relative to the tensor anomalous magnetic moments. Here, we assume the isospin symmetry: $F_{i,T}^{u,n} = F_{i,T}^{d,p}$ and $F_{i,T}^{d,n} = F_{i,T}^{u,p}$ ($i = 1, 2$). Since the nucleon form factors can be approximated as constants within the energy range of CE ν NS, the dependence on the momentum transfer is not explicitly included. After suppressing the lepton flavor label for simplicity, we obtain the effective Lagrangian at the nucleon level:

$$\mathcal{L}_{\text{eff}}^{T,N} = \sum_{N=p,n} \bar{\nu} \sigma^{\mu\nu} \nu \bar{N} \left[G_T^{N,1} \sigma_{\mu\nu} - G_T^{N,2} \frac{i}{m_N} (\gamma^\mu q^\nu - \gamma^\nu q^\mu) \right] N, \quad (3)$$

with nucleon couplings $G_T^{N,i} \equiv \sum_{q=u,d} G_T^q F_{i,T}^{q,N}$ ($i = 1, 2$).

Notice that $F_{2,T}^{q,N}$ and $F_{1,T}^{q,N}$ are at the same order, resulting in a comparable contribution from the tensor charge and the tensor anomalous magnetic moment.

In the nuclear response framework, the cross section is factorized into the leptonic and nuclear parts, where nuclear response functions are determined by non-relativistic (NR) nucleon operators. After performing the following NR expansions of nucleon fermion bilinears, we can match Eqn. 3 with its NR form:

$$\mathcal{L}_{\text{eff}}^{T,\text{NR}} = \sum_{N=p,n} l_0^N 1_N + \bar{l}_5^N \cdot \vec{\sigma}_N + \bar{l}_E^N \cdot \left(-i \frac{\vec{P}_N}{2m_N} \times \vec{\sigma}_N \right), \quad (4)$$

TABLE I. NR expansions of the tensor interactions up to $\mathcal{O}(|\vec{q}|/m_N)$, where $\sigma_{(0)}^i = \sigma^{0i}$, $\sigma_{(1)}^i = \frac{1}{2} \epsilon^{ijk} \sigma^{jk}$ and the state normalization factor $\rho_p \simeq 2M$ with M being the nucleus mass.

	$\vec{T}_{(0)}^1$	$\vec{T}_{(1)}^1$	$\vec{T}_{(0)}^2$
neutrino	$-2\bar{u}_k' \vec{\sigma}_{(0)} u_k$	$2\bar{u}_k' \vec{\sigma}_{(1)} u_k$	$-2\bar{u}_k' \vec{\sigma}_{(0)} u_k$
nucleon	$\frac{i\vec{q} 1_N - \vec{P} \times \vec{\sigma}_N}{2m_N} G_T^{N,1} \rho_p$	$\vec{\sigma}_N G_T^{N,1} \rho_p$	$-\frac{i\vec{q}}{m_N} 1_N G_T^{N,2} \rho_p$
parity	odd	even	odd

where \vec{P}_N is the total momentum operator, and l_0^N , \bar{l}_5^N and \bar{l}_E^N are leptonic charge or currents associated with their corresponding operators. According to the remaining spatial rotational symmetry, the tensor interactions can be decomposed into three vector interactions: $\vec{T}_{(0)}^1$ and $\vec{T}_{(1)}^1$ from the first term and $\vec{T}_{(0)}^2$ from the second term in Eqn. 3. The matching results are listed in Tab. I, with derivation details and explicit expressions of l_0 , \bar{l}_5 and \bar{l}_E provided in the supplemental material. Here the three vector interactions are decomposed into neutrino and nucleon components, and the parity of the nucleon operators are also presented according to their underlying Lorentz structures. Notice that the NR expansions are consistent with their relativistic interaction in terms of parity, since the parity of the dimensionless quantities $\frac{\vec{P}_N}{m_N}$, $\vec{\sigma}_N$ and $\frac{i\vec{q}}{m_N}$ are odd, even and odd, respectively. Therefore, the suppression of 1_N by $|\vec{q}|/m_N$ can be attributed to the necessity of preserving the parity. On the other hand, this factor can also be geometrically interpreted as the rapidity of boosting the initial nucleon to a scattered nucleon.

Since the nucleus is modeled as a composite system, the nucleon operator O_N is accompanied by an additional spatial operator $e^{-i\vec{q}\cdot\vec{x}}$ [39]. The factor $e^{-i\vec{q}\cdot\vec{x}}$ can be done by performing a multipole expansion [48, 49], obtained by expanding the exponential into a series of terms that give rise to spherical tensor operators. The transition reduced nuclear matrix element for the multipole operator, i.e., the nuclear response function, can be evaluated by the large scale shell model. For example, the multipole operator of 1_N is denoted by M_J , where J represents its rank, leading to the nuclear response function $\mathcal{F}_N^{M_J}(|\vec{q}|^2)$. At the long-wavelength limit, 1_N counts the number of nucleons inside the nucleus, leading to $\mathcal{F}_p^{M_0}(0) = Z$ and $\mathcal{F}_n^{M_0}(0) = N$ with the proton number Z and the neutron number N . With the aid of the parity and time reversal properties of multipole operators, we find that only four nuclear response functions remain in our discussion [38, 39, 50]: \mathcal{F}_N^M from 1_N , $\mathcal{F}_N^{\Sigma'}$ and $\mathcal{F}_N^{\Sigma''}$ from the spin operator $\vec{\sigma}_N$, and $\mathcal{F}_N^{\Phi''}$ from the spin-orbit operator $\frac{\vec{P}_N \times \vec{\sigma}_N}{2m_N}$, where the nuclear response function is now denoted by \mathcal{F}_N^O for simplicity. For an evaluation of nuclear response functions, please refer to the supplemental material.

Cross sections. The cross section of the tensor interactions can be derived as in Ref. [39], with further details given in the supplemental material. We find that the differential cross section in terms of the recoil energy E_r is decomposed into P-odd (O) and P-even (E) terms:

$$\frac{d\sigma_T}{dE_r} = \frac{d\sigma_T^O}{dE_r} + \frac{d\sigma_T^E}{dE_r}, \quad (5)$$

where

$$\begin{aligned} \frac{d\sigma_T^O}{dE_r} &= \frac{M}{2\pi} \frac{|\vec{q}|^2}{m_N^2} \sum_{N,N'=p,n} \left(c_0^N c_0^{N'} \mathcal{F}_N^M \mathcal{F}_{N'}^M \right. \\ &\left. + 4c_0^N G_T^{N',1} \mathcal{F}_N^{\Phi''} \mathcal{F}_{N'}^M + 4G_T^{N,1} G_T^{N',1} \mathcal{F}_N^{\Phi''} \mathcal{F}_{N'}^{\Phi''} \right) \left(1 - \frac{E_r}{E_\nu} \right), \end{aligned} \quad (6)$$

with $c_0^N \equiv -G_T^{N,1} + 2G_T^{N,2}$ and

$$\begin{aligned} \frac{d\sigma_T^E}{dE_r} &= \frac{M}{\pi} \sum_{N,N'=p,n} [G_T^{N,1} G_T^{N',1} 2 \left(1 - \frac{E_r}{E_\nu} \right) \mathcal{F}_N^{\Sigma''} \mathcal{F}_{N'}^{\Sigma''} \\ &+ G_T^{N,1} G_T^{N',1} \left(1 - \frac{ME_r}{2E_\nu^2} - \frac{E_r}{E_\nu} \right) \mathcal{F}_N^{\Sigma'} \mathcal{F}_{N'}^{\Sigma'}] \end{aligned} \quad (7)$$

The P-odd cross section is dominated by the $\mathcal{F}_N^M \mathcal{F}_{N'}^M$ term, while the $\mathcal{F}_N^{\Phi''} \mathcal{F}_{N'}^M$ term, arising from the interference between 1_N and the spin-orbit operator, constitutes a significant secondary contribution. This is in contrast to the vector case, where the contribution of the spin-orbit operator can be neglected, e.g., in the evaluation of the weak radius [41, 51]. Qualitatively, the nuclear response functions for P-odd and P-even terms are estimated by the atomic number A and the spin expectation value $\langle \mathbf{S}_N \rangle$ based on their normalizations. The ratio between the two parts can be estimated by $\sigma_T^O/\sigma_T^E \simeq \frac{A^2 |\vec{q}|^2}{m_N^2 \langle \mathbf{S}_N \rangle^2} \gtrsim \mathcal{O}(10)$ for a heavy nucleus with $A \gtrsim 100$, given $|\vec{q}| \sim 10$ MeV, $m_N \sim 1$ GeV and $\langle \mathbf{S}_N \rangle^2 \sim \mathcal{O}(0.1)$ [38, 52, 53]. Consequently, the P-odd part tends to dominate over the P-even part due to its spin-dependent suppression omitted in the NPC procedure. Notice that the results on the tensor interactions in Refs. [40, 41] employ the NPC approach and consider exclusively the contribution from $\vec{\sigma}_N$. We have checked that it is consistent with our P-even cross section; see the supplemental material for detailed derivation.

In addition to the tree-level contributions discussed above, the tensor interactions can naturally induce a neutrino magnetic moment (ν MM) [6, 45]:

$$\mu_\nu^q \approx \frac{m_e N_c}{\pi^2} G_T^q m_q Q_q [1 + \ln(G_T^q m_q^2)] \mu_B, \quad (8)$$

where N_c is the number of quark colors, Q_q is the quark electric charge, μ_B is the Born magnetic moment, m_e and m_q are the electron and quark masses, respectively. The sign of ν MM is flipped for the antineutrino. Note that the tensor interaction induced ν MM (TI- ν MM) depends on

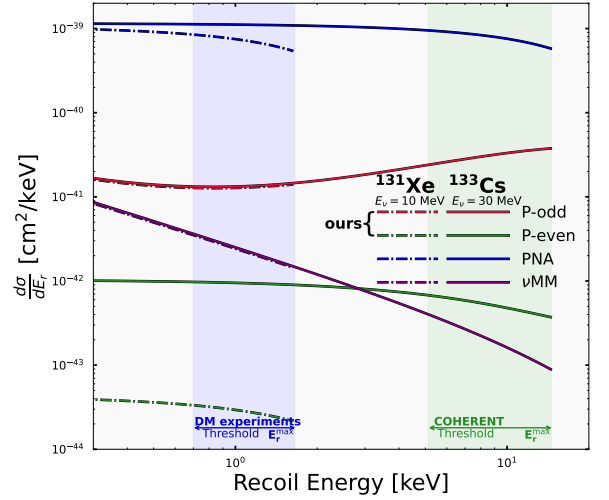


FIG. 1. The differential cross section for ^{133}Cs with an incident neutrino energy at 30 MeV, assuming $G_T^u = G_F$ and $G_T^d = 0$.

the UV behavior of the effective interaction, and could be canceled by other mechanisms that generate ν MM [54, 55]. It is worth highlighting that TI- ν MM would vanish if the neutrino had similar tensor couplings with u and d quarks, due to the cancellation resulting from the opposite electric charges of the two quarks. If we take account of the TI- ν MM, $\frac{d\sigma_T^O}{dE_r}$ in Eqn. 6 is modified with the following replacement:

$$c_0^p \rightarrow -G_T^{p,1} + 2G_T^{p,2} + \frac{m_N}{|\vec{q}|^2} e \sum_{q=u,d} \mu_\nu^q, \quad (9)$$

where e is the electromagnetic coupling constant. Thus, the quadratic contribution of TI- ν MM is proportional to $1/|\vec{q}|^2 \sim 1/E_r$, which dominates at low energies.

Taking ^{133}Cs and ^{131}Xe as benchmark targets, the differential cross section for the tensor interactions with $G_T^u = G_F$ is illustrated in Fig. 1 with G_F being the Fermi constant. The benchmark neutrino energies are 30 MeV and 10 MeV, for a typical muon neutrino energy in the COHERENT experiment and ^8B neutrino energy in the DM experiment, respectively. It is evident that the P-odd contribution predominates the cross section, which is approximately two and three orders of magnitude larger than that from the NPC procedure for ^{133}Cs and ^{131}Xe , respectively. The contribution of ν MM is also demonstrated by deactivating the tree-level contributions due to their interference. The absence of the suppression $|\vec{q}|/m_N$ makes ν MM pronounced for low energy threshold experiments such as DM direct detection experiments. The opposite tensor quark couplings, e.g., $G_T^u = -G_T^d = G_F$, result in a large ν MM and its overwhelming effect. Furthermore, the PNA results are also presented for illustration, which are about an order of magnitude larger than ours.

Experimental constraints. Based on the COHERENT-2021 data [25] and ^8B neutrino observations in the DM direct detection experiments [26, 27], we present the 90% confidence level (CL) constraints on the tensor interactions, as illustrated in Fig. 2. For further details on the spectra and the statistical method, please refer to the supplemental material. The COHERENT-2021 data [25] set the strongest limits on lepton-flavor-independent tensor couplings for CE ν NS experiments. Due to the interference of proton and neutron couplings in Eqn. 5, the cross section diminishes along the direction of the diagonal strip in Fig. 2, leading to the formation of the survival strip. In comparison, the large statistical uncertainties in the DM experiments lead to a less stringent constraint. However, the neutrino oscillation offers a valuable channel to probe τ -flavor tensor couplings, which are inaccessible through the COHERENT experiment. In this context, the neutrino propagation from the Sun to Earth and the matter effect must be included. The relevant result is also presented in Fig. 2, which might facilitate studies on neutrino-related new physics within the neutrino fog [56–59].

Moreover, TI- ν MM can be probed by alternative experiments [54, 55]. Due to its dependence on the energy scale of new physics, a comprehensive examination of ν MM is beyond the scope of this work. For illustration, we present two conservative limits on ν MM derived from COHERENT [60, 61] and XENON-nT [62, 63] experiments. However, due to the opposite electric charges of u and d quarks, TI- ν MM is expected to vanish in the universal coupling scenario. The skew diagonal strip enclosed by two dashed lines in Fig. 2 is permitted by the limits of ν MM but excluded by CE ν NS experiments, thereby indicating that CE ν NS experiments complement ν MM in probing the tensor interactions.

Furthermore, the stringent constraint on tensor interactions arises from the upper limit on the neutrino mass [14, 15], which also depends on the energy scale of new physics. This constraint might be alleviated by incorporating pseudo-scalar interactions or alternative neutrino mass generation mechanisms. Similarly, CE ν NS experiments can exclude the parameter space with opposite couplings for u and d quarks, where the tensor interaction-induced neutrino masses are too small to be constrained by the upper limit on the neutrino mass.

The universal tensor interaction with a light mediator is also demonstrated. To generalize to the light mediator scenario, one can substitute the following replacement in Eqn. 1:

$$G_{T,\alpha}^q \rightarrow \frac{g_T^2}{m_T^2 + |\vec{q}|^2}, \quad (10)$$

where g_T and m_T are the universal tensor coupling and the light mediator mass, respectively. As illustrated in Fig. 3, the green and blue lines delimit the boundaries of the

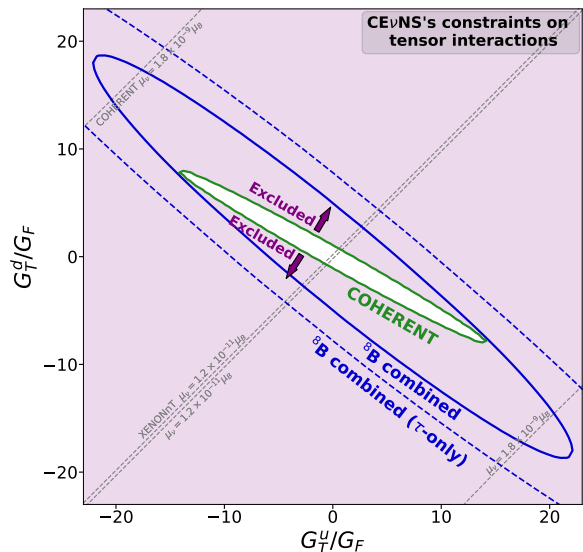


FIG. 2. CE ν NS’s constraints (light purple regions) on neutrino flavor-independent tensor couplings: G_T^u and G_T^d . Blue dashed line represents the constraints on $G_{T,\tau}^u$ and $G_{T,\tau}^d$ for only τ -flavor couplings being nonzero, and the axis labels should be modified accordingly. ^8B combined represents the constraints from the combined data analysis of PandaX-4T and XENONnT.

90% CL excluded regions derived from the COHERENT-2021 data and the DM experiments, respectively. In the high-mass region, the propagator is uniquely determined by m_T since $|\vec{q}| \ll m_T$, leading to diagonal lines proportional to m_T . Conversely, in the low-mass region, the flattens of the boundaries come from the fact that $|\vec{q}| \gg m_T$, indicating that the scattering experiments lose their sensitivities to lighter mediators. DM detectors, with a lower energy threshold, are more sensitive to the smaller momentum transfer compared to COHERENT experiments. Therefore, the DM experiments put more stringent constraints on $m_T \lesssim 30$ MeV. It is undisputed that two types of CE ν NS experiments are complementary in probing neutrino-related new physics. Moreover, we demonstrate the effect of the large uncertainty on nucleon form factors. For example, we vary $F_{2,T}^{u,p}$ within its 1σ region, presenting the results as shaded bands in Fig. 3. The uncertainties of nucleon form factors, particularly for $F_{2,T}^{u,p}$ and $F_{2,T}^{d,p}$, substantially affect the CE ν NS constraints on the tensor interactions. These effects could be mitigated by a more precise evaluation of nucleon form factors in the future. For comparison, we also present the results for the NPC procedure, which are considerably less stringent than those of the full contribution.

Summary. In this work, we pointed out that the conventional SI form factor used in the PNA approach is insufficient to describe the nuclear effect for the tensor interactions. Utilizing the nuclear response framework, we derived the complete expressions for the cross section

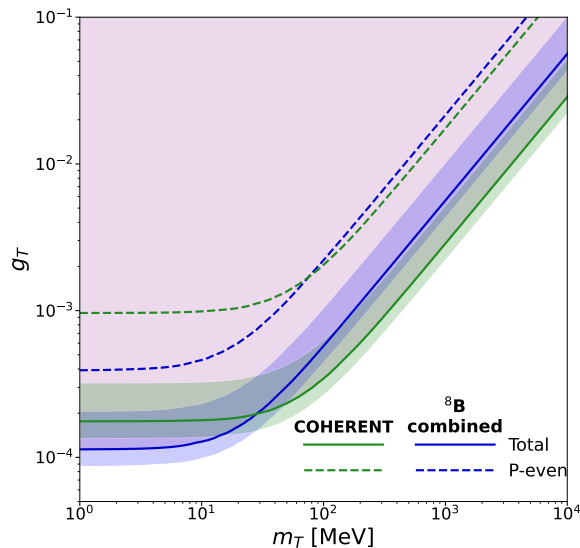


FIG. 3. Constraints on the universal tensor interaction with a light mediator from CE ν NS experiments.

of the tensor interactions that have been overlooked in previous studies. We found that the tensor anomalous magnetic moment plays a role comparable to the tensor charge. Our result revealed that the tensor interactions evade the nuclear spin suppression obtained by the NPC procedure, leading to an enhancement to the cross section by a few orders of magnitude. We systematically incorporated previously omitted TI- ν MM into our discussion.

Employing COHERENT data and recent solar neutrino observations in DM detectors, we demonstrated the complementarity of constraints from CE ν NS and ν MM on the tensor interactions. We also showed that novel solar neutrino observations advance in probing tensor interactions with τ -flavor couplings and a light mediator. Future higher-precision CE ν NS experiments will undoubtedly improve sensitivities in the search of new physics. For tensor interactions, it is also crucial to improve the evaluation of the nucleon form factor. Moreover, our results motivated revised interpretations on CE ν NS experiments using spin-zero nuclei.

Acknowledgments. We appreciate Gang Li, Ning-Qiang Song, Feng-Jie Tang and Jiang-Hao Yu for fruitful discussions. J.T. is supported in part by National Natural Science Foundation of China under Grant Nos. 12347105 and 12075326. J.L. is supported by the National Natural Science Foundation of China under Grant Nos. 12275368 and the Fundamental Research Funds for the Central Universities, Sun Yat-Sen University under Grant No. 24qnp116. This work was supported in part by Fundamental Research Funds for the Central Universities (23xkjc017) in Sun Yat-sen University. J.T. is grateful to Southern Center for Nuclear-Science Theory (SCNT) at Institute of Modern Physics in Chinese Academy of Sciences for hospitality.

REFERENCES

- * Email Address: liaojiajun@mail.sysu.edu.cn.
† Email Address: tangjian5@mail.sysu.edu.cn.
‡ Email Address: zhangblong@mail2.sysu.edu.cn.
- [1] T. D. Lee and C.-N. Yang, Phys. Rev. **104**, 254 (1956).
 - [2] S. Bergmann, Y. Grossman, and E. Nardi, Phys. Rev. D **60**, 093008 (1999), arXiv:hep-ph/9903517.
 - [3] M. Lindner, W. Rodejohann, and X.-J. Xu, JHEP **03**, 097 (2017), arXiv:1612.04150 [hep-ph].
 - [4] D. Aristizabal Sierra, V. De Romeri, and N. Rojas, Phys. Rev. D **98**, 075018 (2018), arXiv:1806.07424 [hep-ph].
 - [5] P. Herczeg, Prog. Part. Nucl. Phys. **46**, 413 (2001).
 - [6] X.-J. Xu, Phys. Rev. D **99**, 075003 (2019), arXiv:1901.00482 [hep-ph].
 - [7] I. Bischer and W. Rodejohann, Nucl. Phys. B **947**, 114746 (2019), arXiv:1905.08699 [hep-ph].
 - [8] T. Han, J. Liao, H. Liu, and D. Marfatia, JHEP **07**, 207 (2020), arXiv:2004.13869 [hep-ph].
 - [9] J. Barranco, A. Bolanos, E. A. Garcés, O. G. Miranda, and T. I. Rashba, Int. J. Mod. Phys. A **27**, 1250147 (2012), arXiv:1108.1220 [hep-ph].
 - [10] F. J. Escrihuela, L. J. Flores, O. G. Miranda, and J. Rendón, JHEP **07**, 061 (2021), arXiv:2105.06484 [hep-ph].
 - [11] F. J. Escrihuela, L. J. Flores, O. G. Miranda, J. Rendón, and R. Sánchez-Vélez, JHEP **04**, 102 (2024), arXiv:2308.15630 [hep-ph].
 - [12] C. A. Gagliardi, R. E. Tribble, and N. J. Williams, Phys. Rev. D **72**, 073002 (2005), arXiv:hep-ph/0509069.
 - [13] A. Hillairet et al. (TWIST), Phys. Rev. D **85**, 092013 (2012), arXiv:1112.3606 [hep-ex].
 - [14] T. M. Ito and G. Prezeau, Phys. Rev. Lett. **94**, 161802 (2005), arXiv:hep-ph/0410254.
 - [15] G. Prezeau and A. Kurylov, Phys. Rev. Lett. **95**, 101802 (2005), arXiv:hep-ph/0409193.
 - [16] A. S. Carnoy, J. Deutsch, T. A. Girard, and R. Prieels, Phys. Rev. C **43**, 2825 (1991).
 - [17] E. G. Adelberger, C. Ortiz, A. Garcia, H. E. Swanson, M. Beck, O. Tengblad, M. J. G. Borge, I. Martel, and H. Bichsel (ISOLDE), Phys. Rev. Lett. **83**, 1299 (1999), [Erratum: Phys.Rev.Lett. 83, 3101 (1999)], arXiv:nucl-ex/9903002.
 - [18] V. Cirigliano, S. Gardner, and B. Holstein, Prog. Part. Nucl. Phys. **71**, 93 (2013), arXiv:1303.6953 [hep-ph].
 - [19] M. González-Alonso, O. Naviliat-Cuncic, and N. Severijns, Prog. Part. Nucl. Phys. **104**, 165 (2019), arXiv:1803.08732 [hep-ph].
 - [20] I. K. Banerjee, U. K. Dey, N. Nath, and S. S. Shariff, JCAP **04**, 002 (2024), arXiv:2304.02505 [hep-ph].
 - [21] M. Aker et al. (KATRIN), (2024), arXiv:2410.13895 [nucl-ex].
 - [22] M. Abdullah et al., (2022), arXiv:2203.07361 [hep-ph].
 - [23] D. Akimov et al. (COHERENT), Science **357**, 1123 (2017), arXiv:1708.01294 [nucl-ex].
 - [24] D. Akimov et al. (COHERENT), Phys. Rev. Lett. **126**, 012002 (2021), arXiv:2003.10630 [nucl-ex].
 - [25] D. Akimov et al. (COHERENT), Phys. Rev. Lett. **129**, 081801 (2022), arXiv:2110.07730 [hep-ex].
 - [26] Z. Bo et al. (PandaX), Phys. Rev. Lett. **133**, 191001 (2024), arXiv:2407.10892 [hep-ex].
 - [27] E. Aprile et al. (XENON), Phys. Rev. Lett. **133**, 191002 (2024), arXiv:2408.02877 [nucl-ex].

- [28] D. Z. Freedman, *Phys. Rev. D* **9**, 1389 (1974).
- [29] D. K. Papoulias and T. S. Kosmas, *Phys. Rev. D* **97**, 033003 (2018), arXiv:1711.09773 [hep-ph].
- [30] D. Aristizabal Sierra, J. Liao, and D. Marfatia, *JHEP* **06**, 141 (2019), arXiv:1902.07398 [hep-ph].
- [31] T. Li, X.-D. Ma, and M. A. Schmidt, *JHEP* **07**, 152 (2020), arXiv:2005.01543 [hep-ph].
- [32] W.-F. Chang and J. Liao, *Phys. Rev. D* **102**, 075004 (2020), arXiv:2002.10275 [hep-ph].
- [33] M. Demirci and M. F. Mustamin, in *Beyond Standard Model: From Theory to Experiment* (2021).
- [34] L. J. Flores, N. Nath, and E. Peinado, *Phys. Rev. D* **105**, 055010 (2022), arXiv:2112.05103 [hep-ph].
- [35] A. Majumdar, D. K. Papoulias, and R. Srivastava, *Phys. Rev. D* **106**, 013001 (2022), arXiv:2112.03309 [hep-ph].
- [36] V. De Romeri, O. G. Miranda, D. K. Papoulias, G. Sanchez Garcia, M. Tórtola, and J. W. F. Valle, *JHEP* **04**, 035 (2023), arXiv:2211.11905 [hep-ph].
- [37] S. S. Chatterjee, S. Lavignac, O. G. Miranda, and G. Sanchez Garcia, *Phys. Rev. D* **110**, 095027 (2024), arXiv:2402.16953 [hep-ph].
- [38] A. L. Fitzpatrick, W. Haxton, E. Katz, N. Lubbers, and Y. Xu, *JCAP* **02**, 004 (2013), arXiv:1203.3542 [hep-ph].
- [39] N. Anand, A. L. Fitzpatrick, and W. C. Haxton, *Phys. Rev. C* **89**, 065501 (2014), arXiv:1308.6288 [hep-ph].
- [40] W. Altmannshofer, M. Tammaro, and J. Zupan, *JHEP* **09**, 083 (2019), [Erratum: *JHEP* **11**, 113 (2021)], arXiv:1812.02778 [hep-ph].
- [41] M. Hoferichter, J. Menéndez, and A. Schwenk, *Phys. Rev. D* **102**, 074018 (2020), arXiv:2007.08529 [hep-ph].
- [42] P. M. Candela, V. De Romeri, P. Melas, D. K. Papoulias, and N. Saoulidou, *JHEP* **10**, 032 (2024), arXiv:2404.12476 [hep-ph].
- [43] V. De Romeri, D. K. Papoulias, and C. A. Ternes, (2024), arXiv:2411.11749 [hep-ph].
- [44] A. Chattaraj, A. Majumdar, D. K. Papoulias, and R. Srivastava, (2025), arXiv:2501.12443 [hep-ph].
- [45] D. K. Papoulias and T. S. Kosmas, *Phys. Lett. B* **747**, 454 (2015), arXiv:1506.05406 [hep-ph].
- [46] R. Gupta, B. Yoon, T. Bhattacharya, V. Cirigliano, Y.-C. Jang, and H.-W. Lin, *Phys. Rev. D* **98**, 091501 (2018), arXiv:1808.07597 [hep-lat].
- [47] M. Hoferichter, B. Kubis, J. Ruiz de Elvira, and P. Stoffer, *Phys. Rev. Lett.* **122**, 122001 (2019), [Erratum: *Phys.Rev.Lett.* **124**, 199901 (2020)], arXiv:1811.11181 [hep-ph].
- [48] T. W. Donnelly and W. C. Haxton, *Atom. Data Nucl. Data Tabl.* **23**, 103 (1979).
- [49] W. Haxton and C. Lunardini, *Comput. Phys. Commun.* **179**, 345 (2008), arXiv:0706.2210 [nucl-th].
- [50] E. Del Nobile, (2021), 10.1007/978-3-030-95228-0, arXiv:2104.12785 [hep-ph].
- [51] P. Coloma, I. Esteban, M. C. Gonzalez-Garcia, and J. Menendez, *JHEP* **08**, 030 (2020), arXiv:2006.08624 [hep-ph].
- [52] P. Klos, J. Menéndez, D. Gazit, and A. Schwenk, *Phys. Rev. D* **88**, 083516 (2013), [Erratum: *Phys.Rev.D* **89**, 029901 (2014)], arXiv:1304.7684 [nucl-th].
- [53] B. S. Hu, J. Padua-Argüelles, S. Leutheusser, T. Miyagi, S. R. Stroberg, and J. D. Holt, *Phys. Rev. Lett.* **128**, 072502 (2022), arXiv:2109.00193 [nucl-th].
- [54] C. Giunti and A. Studenikin, *Rev. Mod. Phys.* **87**, 531 (2015), arXiv:1403.6344 [hep-ph].
- [55] C. Giunti, K. Kouzakov, Y.-F. Li, and A. Studenikin, (2024), 10.1146/annurev-nucl-102122-023242, arXiv:2411.03122 [hep-ph].
- [56] C. A. J. O'Hare, *Phys. Rev. Lett.* **127**, 251802 (2021), arXiv:2109.03116 [hep-ph].
- [57] J. Tang and B.-L. Zhang, *Phys. Rev. D* **108**, 062004 (2023), arXiv:2304.13665 [hep-ph].
- [58] J. Tang and B.-L. Zhang, *JHEP* **12**, 074 (2024), arXiv:2403.05819 [hep-ph].
- [59] P. Blanco-Mas, P. Coloma, G. Herrera, P. Huber, J. Kopp, I. M. Shoemaker, and Z. Tabrizi, (2024), arXiv:2411.14206 [hep-ph].
- [60] P. Coloma, I. Esteban, M. C. Gonzalez-Garcia, L. Larizgoitia, F. Monrabal, and S. Palomares-Ruiz, *JHEP* **05**, 037 (2022), arXiv:2202.10829 [hep-ph].
- [61] M. Atzori Corona, M. Cadeddu, N. Cargioli, F. Dordei, C. Giunti, Y. F. Li, C. A. Ternes, and Y. Y. Zhang, *JHEP* **09**, 164 (2022), arXiv:2205.09484 [hep-ph].
- [62] A. N. Khan, *Phys. Lett. B* **837**, 137650 (2023), arXiv:2208.02144 [hep-ph].
- [63] S. K. A., A. Majumdar, D. K. Papoulias, H. Prajapati, and R. Srivastava, *Phys. Lett. B* **839**, 137742 (2023), arXiv:2208.06415 [hep-ph].
- [64] A. L. Fetter, J. D. Walecka, and L. P. Kadanoff, *Quantum Theory of Many-Particle Systems* (1971).
- [65] J. S. O'Connell, T. W. Donnelly, and J. D. Walecka, *Phys. Rev. C* **6**, 719 (1972).
- [66] J. D. Walecka, *Theoretical Nuclear And Subnuclear Physics* (World Scientific, 2001).
- [67] T. W. Donnelly and I. Sick, *Rev. Mod. Phys.* **56**, 461 (1984).
- [68] J. Menendez, A. Poves, E. Caurier, and F. Nowacki, *Nucl. Phys. A* **818**, 139 (2009), arXiv:0801.3760 [nucl-th].
- [69] O. C. Gorton, C. W. Johnson, C. Jiao, and J. Nikoļeyczik, *Comput. Phys. Commun.* **284**, 108597 (2023), arXiv:2209.09187 [nucl-th].
- [70] R. Abdel Khaleq, G. Busoni, C. Simenel, and A. E. Stuchbery, *Phys. Rev. D* **109**, 075036 (2024), arXiv:2311.15764 [hep-ph].
- [71] R. Abdel Khaleq, J. L. Newstead, C. Simenel, and A. E. Stuchbery, (2024), arXiv:2405.20060 [hep-ph].
- [72] J. N. Bahcall, A. M. Serenelli, and S. Basu, *Astrophys. J. Lett.* **621**, L85 (2005), arXiv:astro-ph/0412440.
- [73] J. Bergstrom, M. C. Gonzalez-Garcia, M. Maltoni, C. Pena-Garay, A. M. Serenelli, and N. Song, *JHEP* **03**, 132 (2016), arXiv:1601.00972 [hep-ph].
- [74] D. Aristizabal Sierra, N. Mishra, and L. Strigari, (2024), arXiv:2409.02003 [hep-ph].
- [75] G. Li, C.-Q. Song, F.-J. Tang, and J.-H. Yu, *Phys. Rev. D* **111**, 035002 (2025), arXiv:2409.04703 [hep-ph].
- [76] E. Vitagliano, I. Tamborra, and G. Raffelt, *Rev. Mod. Phys.* **92**, 45006 (2020), arXiv:1910.11878 [astro-ph.HE].

SUPPLEMENTAL MATERIAL

A. Nuclear response

To evaluate the nuclear response functions, one needs to deal with the many-body calculation. Fortunately, the traditional non-relativistic many-body description of the nucleus has been developed in Ref. [64]. The nucleus is modeled as a quantum mechanical system of point nucleons, where each nucleon is described by a single-particle Hartree-Fock state with a definite nodal number and angular momentum. For a single-nucleon multipole operator O_N^J , which is an irreducible tensor operator with rank J , the transition reduced nuclear matrix element between initial and final nuclear many-body states Ψ_i and Ψ_f reads [65, 66]:

$$\langle \Psi_f | \hat{O}_N^J | \Psi_i \rangle = \sum_{\alpha, \beta} \langle \alpha | O_N^J | \beta \rangle \psi_{\alpha\beta}^{fi}, \quad (11)$$

where \hat{O}_N^J is the second quantization version of O_N^J , and $|\alpha\rangle, |\beta\rangle$ represents the single-particle Hartree-Fock state. The single-nucleon matrix element $\langle \alpha | O_N^J | \beta \rangle$ can be evaluated analytically in a harmonic oscillator single-particle basis, yielding a form like $e^{-\frac{u}{2}} p(u)$, where $p(u)$ is a polynomial in $u = |\vec{q}|^2 b^2 / 2$ with the oscillator parameter b and the three-momentum transfer $|\vec{q}|$ [48, 49, 67]. The one-body density matrix element $\psi_{\alpha\beta}^{fi}$, generated by performing a large-scale nuclear shell model calculation, encodes the many-body physics. For isotopes (^{127}I , ^{133}Cs , ^{131}Xe , etc.) discussed in this work, we adopt GCN5082 [68] as the shell model interaction. The calculation of the reduced nuclear matrix element can be readily generated by **dmformfactor** [39]¹. In CE ν NS, we define the nuclear response function:

$$\mathcal{F}_N^{O_N^J}(\mathbf{q}^2) \equiv \sqrt{\frac{4\pi}{2J_i + 1}} \langle | \hat{O}_N^J | | \rangle = \sqrt{\frac{4\pi}{2J_i + 1}} e^{-\frac{u}{2}} \sum_j c_j^{O_N^J} u^j, \quad (12)$$

where $| \rangle$ is the nuclear ground state, J_i is the angular momentum of the ground state and the coefficients $c_j^{O_N^J}$ can be derived analytically. We always suppress the rank label and the nuclear response function is denoted by $\mathcal{F}_N^O(\mathbf{q}^2)$ for simplicity. Note that the uncertainty in the crucial nuclear response function \mathcal{F}_N^M can be disregarded [70, 71]. In addition, we provide a python script for the evaluation of the nuclear response functions and the cross section of the tensor interactions².

B. Details of cross section calculations

The procedure of the NR expansion on the tensor interactions is now introduced. Kinematics of CE ν NS is defined by: $\nu(k) + \mathcal{N}(p) \rightarrow \nu(k') + \mathcal{N}(p')$, with $q \equiv k' - k = p - p'$. At the NR limit, the Weyl spinor for a nucleon reads: $u^s(p) = \frac{1}{\sqrt{4m_N}} \begin{pmatrix} (2m_N - \vec{p} \cdot \vec{\sigma}) \xi^s \\ (2m_N + \vec{p} \cdot \vec{\sigma}) \xi^s \end{pmatrix}$, with a helicity s ³. Thus, nucleon fermion bilinears $\bar{u}(p') \Gamma u(p)$ can be computed accordingly, where Γ represents the Lorentz structure of the interaction and the helicity s is suppressed. It is worth emphasizing that a nuclear state $\mathcal{N}(p)$ can be factored as $|\mathcal{N}(p)\rangle = |p\rangle \otimes |\mathcal{N}_{\text{int}}\rangle$, where $|p\rangle$, normalized by $\rho_p = \langle p|p\rangle \simeq 2M$, is an overall nuclear motion state and $|\mathcal{N}_{\text{int}}\rangle$ is a many-body state describing solely the internal nuclear state with a definite total angular momentum [50]. Thus, an additional factor $\frac{2M}{2m_N}$ is necessitated when we consider the transformation between quantized volumes of a nuclear state and a nucleon state. According to the spatial rotational symmetry, we have $\bar{\nu} \sigma^{\mu\nu} \nu \bar{N} \sigma_{\mu\nu} N = -2 \left(\bar{\nu} \sigma_{(0)}^i \nu \bar{N} \sigma_{(0)}^i N - \bar{\nu} \sigma_{(1)}^i \nu \bar{N} \sigma_{(1)}^i N \right)$, with $\sigma_{(0)}^i = \sigma^{0i} = -i \begin{pmatrix} \sigma_i & 0 \\ 0 & -\sigma_i \end{pmatrix}$ and $\sigma_{(1)}^i = \frac{1}{2} \epsilon^{ijk} \sigma^{jk} = \begin{pmatrix} \sigma_i & 0 \\ 0 & \sigma_i \end{pmatrix}$. For the second term in Eqn. 3, we have: $\bar{\nu} \sigma^{\mu\nu} \nu \bar{N} (\gamma^\mu q^\nu - \gamma^\nu q^\mu) N \simeq -2 \bar{\nu} \sigma_{(0)}^i \nu \bar{N} \gamma^0 q^i N$. Other terms are suppressed by $\mathcal{O}((|\vec{q}|/m_N)^2)$, which can be safely neglected. The results of the NR expansion are

¹ Updated single nucleon density matrix elements can be found in **dmscatter**[69] and <https://github.com/Berkeley-Electroweak-Physics/Elastic>.

² <https://github.com/zhangblong/CEvNSTensor>.

³ We following the convention in Ref. [50], while some literature [39, 41] adopt Bjorken and Drell γ matrix conventions and spinor normalization (1 instead of the $2m_N$).

listed in Tab. I. Then one can read out the leptonic components in Eqn. 4:

$$\begin{aligned} l_0^N &= \bar{u}_{k'} \left[-2 \left(G_T^{N,1} - 2G_T^{N,2} \right) \frac{i|\vec{q}|}{2m_N} \right] \sigma_{(0)}^3 u_k \rho_p, \\ \vec{l}_5^N &= \bar{u}_{k'} \left(2G_T^{N,1} \vec{\sigma}_{(1)} \right) u_k \rho_p, \quad \vec{l}_E^N = \bar{u}_{k'} \left(2iG_T^{N,1} \vec{\sigma}_{(0)} \right) u_k \rho_p, \end{aligned} \quad (13)$$

with the state normalization factor $\rho_p \simeq 2M$.

Through the matching between the nucleon operators and the nuclear response functions, the averaged squared amplitude $|\overline{\mathcal{M}}|^2$ for Eqn. 4 reads [39]:

$$\begin{aligned} |\overline{\mathcal{M}}|^2 &= \sum_{N,N'} \{ l_0^N l_0^{N'*} \mathcal{F}_N^M \mathcal{F}_{N'}^M + \frac{|\vec{q}|^2}{m_N^2} l_{E,3}^N l_{E,3}^{N'*} \mathcal{F}_N^{\Phi''} \mathcal{F}_{N'}^{\Phi''} + 2 \frac{|\vec{q}|}{m_N} \text{Re} \left[l_0^N l_{E,3}^{N'*} \right] \mathcal{F}_N^{\Phi''} \mathcal{F}_{N'}^M \\ &\quad l_{5,3}^N l_{5,3}^{N'*} \mathcal{F}_N^{\Sigma''} \mathcal{F}_{N'}^{\Sigma''} + \frac{1}{2} \left(\vec{l}_5^N \cdot \vec{l}_5^{N'*} - l_{5,3}^N l_{5,3}^{N'*} \right) \mathcal{F}_N^{\Sigma'} \mathcal{F}_{N'}^{\Sigma'} \}, \end{aligned} \quad (14)$$

where the transverse contribution of \vec{l}_E^N , proportional to $\mathcal{F}_N^{\Phi'} \mathcal{F}_{N'}^{\Phi'}$, is neglected. Recovering the rank label, terms like $\mathcal{F}_N^M \mathcal{F}_{N'}^M$ should be understood as the incoherent sum of the contributions of the multipole operators with different J : $\mathcal{F}_N^M \mathcal{F}_{N'}^M = \sum_J \mathcal{F}_N^{MJ} \mathcal{F}_{N'}^{MJ}$, since operators with different J are orthogonal. The rank of multipole operators must satisfy a triangular in-equation $0 \leq J \leq 2J_i$ from the Wigner-Eckart theorem. In the low-energy process, rank 0 operators without a $\mathcal{O}((|\vec{q}|/m_N)^J)$ suppression always dominate. The next is to evaluate the leptonic parts in Eqn. 14. For example, considering the incident left-handed neutrino, we have $l_0^N l_0^{N'*} = \text{Tr} \left[k_2 \tilde{\Gamma}_0^N P_L k_1 \tilde{\Gamma}_0^{N'\dagger} \right]$, where $\tilde{\Gamma}_0^N$ is an abbreviation of Eqn. 13. Expanding the leptonic parts up to the next leading order, we have:

$$\begin{aligned} l_0^N l_0^{N'*} &= c_0^N c_0^{N'} \frac{|\vec{q}|^2}{m_N^2} 4E_\nu^2 \left(1 - \frac{E_r}{E_\nu} \right) \rho_p^2 \\ \text{Re} \left[l_0^N l_{E,3}^{N'*} \right] &= c_0^N G_T^{N',1} \frac{|\vec{q}|}{m_N} 8E_\nu^2 \left(1 - \frac{E_r}{E_\nu} \right) \rho_p^2 \\ l_{E,3}^N l_{E,3}^{N'*} &= l_{5,3}^N l_{5,3}^{N'*} = G_T^{N,1} G_T^{N',1} 16E_\nu^2 \left(1 - \frac{E_r}{E_\nu} \right) \rho_p^2 \\ \frac{1}{2} \left(\vec{l}_5^N \cdot \vec{l}_5^{N'*} - l_{5,3}^N l_{5,3}^{N'*} \right) &= G_T^{N,1} G_T^{N',1} 8E_\nu^2 \left(1 - \frac{ME_r}{2E_\nu^2} - \frac{E_r}{E_\nu} \right) \rho_p^2 \\ \frac{1}{2} \left(\vec{l}_E^N \cdot \vec{l}_E^{N'*} - l_{E,3}^N l_{E,3}^{N'*} \right) &= \frac{1}{2} \left(\vec{l}_5^N \cdot \vec{l}_5^{N'*} - l_{5,3}^N l_{5,3}^{N'*} \right), \end{aligned} \quad (15)$$

where $\rho_p = 2M$ and $l_{\alpha,3}^N$ ($\alpha = 5, E$) are the longitudinal component. Note that the longitudinal direction is aligned with \vec{q} . Given $\frac{d\sigma}{dE_r} = \frac{1}{32\pi M E_\nu^2} |\overline{\mathcal{M}}|^2$, we finally obtain Eqn. 5.

C. Cross-check with NPC results

Here, we present how to recover the cross section in the NPC procedure [41] with Eqn. 7. According to the convention in Ref. [41], we define four column matrices: $g^{01} = (g_{T,1}^0 \ g_{T,1}^1)^T$, $g^{pn} = (g_{T,1}^p \ g_{T,1}^n)^T$, $\mathcal{F}^{\Sigma',\pm} = (\mathcal{F}_+^{\Sigma'} \ \mathcal{F}_-^{\Sigma'})^T$, and $\mathcal{F}^{\Sigma',pn} = (\mathcal{F}_p^{\Sigma'} \ \mathcal{F}_n^{\Sigma'})^T$. Note that in this convention, $F_{\Sigma'}^N(0) = \sqrt{\frac{2}{3}} \sqrt{\frac{(2J_i+1)(J_i+1)}{4\pi J_i}} \langle S_N \rangle$. The transition from the nucleon basis to the isospin basis can then be expressed readily: $g_i^{01} = \sum_j \mathbf{O}_{ij} g_j^{pn}$ and $\mathcal{F}_i^{\Sigma',\pm} = \sum_j \mathbf{O}_{ij}^{-1} \mathcal{F}_j^{\Sigma',pn}$, with $\mathbf{O} = \frac{1}{2} \begin{pmatrix} 1 & 1 \\ 1 & -1 \end{pmatrix} = \frac{1}{2} \mathbf{O}^{-1} = \mathbf{O}^T$, leading to a useful relation: $\sum_i g_i^{pn} \mathcal{F}_i^{\Sigma',pn} = \sum_i g_i^{01} \mathcal{F}_i^{\Sigma',\pm}$. In our conventions, $G_{T,1}^N = g_{T,1}^N$, and $F_{\Sigma'}^N(0) = \sqrt{\frac{8(J_i+1)}{3J_i}} \langle S_N \rangle$ [50]. Thus a replacement $F_{\Sigma'}^{\Sigma'} \rightarrow F_{\Sigma'}^{\Sigma'} \sqrt{\frac{16\pi}{2J_i+1}}$ should be included when

converting our result into others. For the term proportional to $\mathcal{F}_N^{\Sigma'} \mathcal{F}_N^{\Sigma'}$, we have:

$$\begin{aligned} \frac{M}{\pi} \sum_{i,j} g_i^{pn} \mathcal{F}_i^{\Sigma',pn} g_j^{pn} \mathcal{F}_j^{\Sigma',pn} \left(1 - \frac{ME_r}{2E_\nu^2} - \frac{E_r}{E_\nu}\right) &= \frac{16M}{2J_i+1} \sum_{i,j} g_i^{01} \mathcal{F}_i^{\Sigma',\pm} g_j^{01} \mathcal{F}_j^{\Sigma',\pm} \left(1 - \frac{ME_r}{2E_\nu^2} - \frac{E_r}{E_\nu}\right) \\ &= \frac{16M}{2J_i+1} \left(1 - \frac{ME_r}{2E_\nu^2} - \frac{E_r}{E_\nu}\right) \left[(g_{T,1}^0)^2 \bar{S}_{00}^T + g_{T,1}^0 g_{T,1}^1 \bar{S}_{01}^T + (g_{T,1}^1)^2 \bar{S}_{11}^T \right], \end{aligned} \quad (16)$$

where the left hand side is from Eqn. 7, and we use the relation: $\bar{S}_{00}^T = \left(\mathcal{F}_+^{\Sigma'}\right)^2$, $\bar{S}_{11}^T = \left(\mathcal{F}_-^{\Sigma'}\right)^2$ and $\bar{S}_{01}^T = 2\mathcal{F}_+^{\Sigma'} \mathcal{F}_-^{\Sigma'}$. This yields the same transverse contribution of Eqn. 108 in Ref. [41]. The longitudinal one can be done in the same way:

$$\frac{M}{\pi} \sum_{i,j} g_i^{pn} \mathcal{F}_i^{\Sigma',pn} g_j^{pn} \mathcal{F}_j^{\Sigma',pn} 2 \left(1 - \frac{E_r}{E_\nu}\right) = \frac{32M}{2J_i+1} \left(1 - \frac{E_r}{E_\nu}\right) \left[(g_{T,1}^0)^2 \bar{S}_{00}^L + g_{T,1}^0 g_{T,1}^1 \bar{S}_{01}^L + (g_{T,1}^1)^2 \bar{S}_{11}^L \right]. \quad (17)$$

D. Experimental analysis

The total differential cross section for isotope i reads:

$$\frac{d\sigma_i}{dE_r} = \frac{d\sigma_{i,SM}}{dE_r} + \frac{d\sigma_{i,T}}{dE_r}, \quad (18)$$

where $\frac{d\sigma_{i,T}}{dE_r}$ presented in Eqn. 5, and $\frac{d\sigma_{i,SM}}{dE_r}$ is taken from Ref. [41]:

$$\frac{d\sigma_{i,SM}}{dE_r} = \frac{G_F^2 M}{4\pi} \left(1 - \frac{ME_r}{2E_\nu^2}\right) Q_w^2 F_w (|\vec{q}|^2)^2, \quad (19)$$

where $Q_w = Z(1 - 4\sin^2\theta_W) - N$ is the weak charge, and F_w is the weak charge distribution inside the nucleus [41]. Note that the form factor parametrization is inconsequential for current CE ν NS experiments, yet it will become relevant for future high-precision CE ν NS experiments [30].

In COHERENT, the low-energy neutrino fluxes are generated at the Spallation Neutron Source (SNS) at the Oak Ridge National Laboratory. The neutrino fluxes consist of monochromatic ν_μ coming from π^+ decays, $\pi^+ \rightarrow \mu^+ \nu_\mu$, along with delayed ν_e and $\bar{\nu}_\mu$ from the subsequent μ^+ decays, $\mu^+ \rightarrow e^+ \bar{\nu}_\mu \nu_e$. Convoluting the differential cross section with neutrino fluxes Φ_α , the differential rates for the CsI detector reads:

$$\frac{dR_{CsI}}{dE_r} = \sum_{i=Cs,I} \sum_{\alpha} \frac{1}{M_i} \int_{E_\nu^{\min}}^{E_\nu^{\max}} \frac{d\Phi_\alpha}{dE_\nu} \frac{d\sigma_i}{dE_r} dE_\nu, \quad (20)$$

where $E_\nu^{\min} \simeq \sqrt{ME_r/2}$, $E_\nu^{\max} = m_\mu/2 = 52.8$ MeV, M_i is the isotope mass, and summations are over $\alpha = \nu_\mu, \nu_e, \bar{\nu}_\mu$. To accurately predict the total events in the CsI detector as a function of the reconstructed energy E_{rec} in units of PE, quenching, energy smearing and detection efficiency must be taken into account. A empirically parameterized quenching $E_{ee} = E_{ee}(E_r)$ builds the relationship between the nuclear recoil energy T and the true quenched energy deposition E_{ee} . Considering the energy smearing $P(E_{\text{rec}}, E_{ee})$ and the efficiency $\varepsilon_E(E_{\text{rec}})$, we have the differential recoil spectrum as a function of E_{rec} :

$$\frac{dR}{dE_{\text{rec}}} = \int dE_{ee} P(E_{\text{rec}}, E_{ee}) \frac{dE_r}{dE_{ee}} \frac{dR_{CsI}}{dE_r}. \quad (21)$$

In addition, because the reconstructed energy and time are uncorrelated, we simply convolute the time information with the time efficiency given by Ref. [25], leading to $\epsilon_{\nu_\mu}^t = 0.997$, $\epsilon_{\bar{\nu}_\mu}^t = 0.848$ and $\epsilon_{\nu_e}^t = 0.848$. Neutrino fluxes, quenching, energy smearing and detection efficiency can be found in the supplementary material of Ref. [25]. For the COHERENT-2021 data, we adopt the following χ^2 :

$$\chi_{\text{COHE.}}^2 = \min_{\alpha,\beta} \left\{ \sum_{i=2}^8 \left[\frac{N_{\text{meas}}^i - (1+\alpha)N_{\text{th}}^i - (1+\beta)B_{\text{on}}^i}{\sigma_{\text{stat}}^i} \right]^2 + \left(\frac{\alpha}{\sigma_\alpha} \right)^2 + \left(\frac{\beta}{\sigma_\beta} \right)^2 \right\}, \quad (22)$$

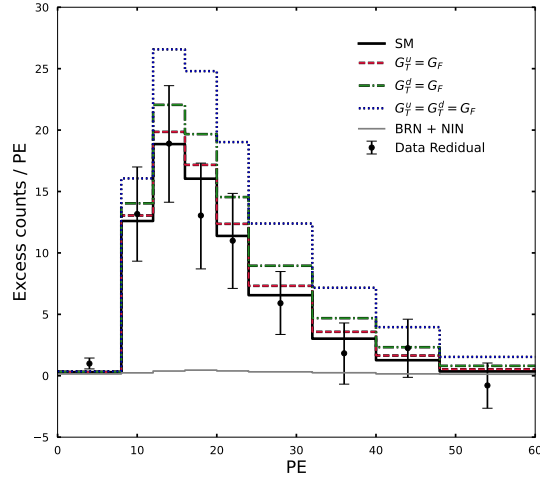


FIG. 4. COHERENT-2021 data and theoretical predicted spectra.

Dataset	Energy range [keV]	N_{meas}	N_{th}
PandaX-4T (paired)	[1.1, 3.0]	3.5 ± 1.3	2.4
PandaX-4T (US2)	[0.3, 3.0]	75 ± 28	44.3
XENONnT	[0.5, 3.0]	10.7 ± 3.95	11.2

TABLE II. Measurements on ${}^8\text{B}$ from PandaX (paired and US2) and XENON experiments.

where N_{meas}^i is the measured number of events per energy bin, B_{on}^i is the beam-on background, N_{th}^i is the theoretical predicted number of events per energy bin in presence of the tensor interactions, σ_{stat}^i is the statistical uncertainty per energy bin, $\sigma_{\alpha} = 0.1195$ is the total systematic uncertainty, and $\sigma_{\beta} = 0.25$ is the the systematic uncertainty for the background. N_{th}^i are derived by integrating Eqn. 21 over the energy bin i . We present the data and theoretical spectra in Fig. 4.

The differential event rates for a Xenon-based detector reads:

$$\frac{dR_{\text{Xe}}}{dE_r} = \sum_i \sum_{\alpha=\epsilon,\mu,\tau} \frac{1}{M_i} \int_{E_{\nu}^{\text{min}}}^{E_{\nu}^{\text{max}}} \left[\int^{R_{\odot}} \frac{d^2\Phi_{\text{sB}}}{dE_{\nu}dr} P_{e\alpha}(r) dr \right] \frac{d\sigma_{i,\nu\alpha}}{dE_r} dE_{\nu}, \quad (23)$$

where $P_{e\alpha}$ denotes the neutrino survival probability from the Sun to the Earth, r is the solar neutrino production position, R_{\odot} represents the solar radius, and the summation spans naturally occurring xenon isotopes in the xenon-based detector, weighted by their terrestrial abundances: ${}^{128}\text{Xe}$ (1.92%), ${}^{129}\text{Xe}$ (26.44%), ${}^{130}\text{Xe}$ (4.08%), ${}^{131}\text{Xe}$ (21.18%), ${}^{132}\text{Xe}$ (26.89%), ${}^{134}\text{Xe}$ (10.44%), and ${}^{136}\text{Xe}$ (8.87%). The ${}^8\text{B}$ neutrino flux $\frac{d^2\Phi_{\text{sB}}}{dE_{\nu}dr}$ is taken from BS05 standard solar model [72], with a normalization factor of $5.16 \times 10^6 \text{ cm}^{-2}\text{s}^{-1}$ from the global fits of neutrino data [73]. In the scenario of the τ -only tensor interaction, the matter effect in the neutrino propagation has been taken into account. Since the tensor interactions only affect the neutrino propagation in a polarized medium [2], the matter effect is exclusively determined by the SM weak interaction. For non-standard neutrino vector interactions, their influence on the neutrino propagation should be incorporated [74, 75]. Therefore, the neutrino survival probability can be evaluated by:

$$P_{\alpha\beta}(r) = \sum_k |U_{\alpha k}^{\text{mat.}}(r)|^2 |U_{\beta k}^{\text{PMNS}}|^2, \quad (24)$$

where U^{PMNS} is the PMNS matrix and $U^{\text{mat.}}$ can be generated by diagonalize the SM matter effect Hamiltonian. One more step to derive the theoretical predicted ${}^8\text{B}$ event numbers is to convolute Eqn. 23 with the efficiencies from PandaX and XENONnT experiments [26, 27]. Three measurements are listed in Tab. II, as well as our SM predictions. The χ^2 for ${}^8\text{B}$ observations is defined by:

$$\chi_{\text{sB}}^2 = \min_{\alpha} \left\{ \sum_j \left[\frac{N_{\text{meas}}^j - (1 + \alpha)N_{\text{th}}^j}{\sigma_{\text{stat}}^j} \right]^2 + \left(\frac{\alpha}{\sigma_{\alpha}} \right)^2 \right\}, \quad (25)$$

where j labels the dataset in Tab. II. Analogous to COHERENT-CsI data, we set $\sigma_\alpha = 0.12$ to account for the systematic uncertainty, originating from the prediction of the neutrino flux [76]. According to Tab. II, the statistical uncertainties for three datasets are 37.1%, 37.3% and 36.9%, respectively.